Materials Research. 2016; 19(3): 648-653
DOI:http://dx.doi.org/10.1590/1980-5373-MR-2016-0006

Dip coating of a carbon steel sheet with Ni reinforced TiO_2 nanoparticles

Luiz Eloi Vieira Junior[a]*****, ***Keila Christina Kleinjohann***[a], ***João Batista Rodrigues Neto***[a]***;***
Aloísio Nelmo Klein[a], ***Dachamir Hotza***[b], ***Rodrigo Moreno***[c]

[a] *Department of Mechanical Engineering, Federal University of Santa Catarina – UFSC, Brazil*
[b] *Department of Chemical Engineering, Federal University of Santa Catarina – UFSC, Brazil*
[c] *Institute of Ceramics and Glass, Consejo Superior de Investigaciones Científicas – CSIC, Spain*

Received: January 5, 2016; Revised: January 29, 2016; Accepted: March 11, 2016

In this work carbon steel plates were dip-coated with a composite film obtained from a colloidal suspension of Ni-TiO_2. Suspensions with different solids contents were used to evaluate the adherence of the film and the microstructural features. The samples were characterized using both optical and scanning electron microscopy, energy dispersive spectroscopy and microhardness. The microstructural analysis revealed that the films have high porosity at the surface. However, an interfacial region was observed demonstrating that there was good adhesion between both materials. This region shows an increased hardness that can be attributed to diffusion mechanism of nickel from the composite film to the steel matrix. Besides the interface, there was an abnormal grain growth, followed by a region of smaller grains of austenite and at longer distances near the center of the plate some colonies of pearlite appear.

Keywords: *Rheology, Metal oxide composite coatings, Dipping*

Background

The processing of materials from powders has several advantages over deformation methods such as the easy tailoring of the microstructure, the adequate control of chemical composition and the possibility to produce ceramic-metal composites. However, the production steps comprising the preparation of raw materials (powders + additives), forming, sintering, calibration, and limitations regarding with the size and geometry of the components makes powder processing to be a complex process with enhanced cost at any stage, which limits the choice of this route[1]. Within this context, there are several techniques for obtaining metallic and ceramic components, the main being pressing, extrusion, forging and other metallurgical techniques that are performed under dry conditions. However, another feasible route for the production of complex parts with uniform microstructures is those based on colloidal routes[2, 3.]

Colloidal processing comprises the preparation of a homogeneous mixture of powders in a liquid medium (organic or preferably water) to form a stable suspension where the repulsive forces impede the tendency to agglomerate due to van der Waals forces keeping the particles well dispersed in the suspension. Some popular techniques for shaping powders into bulk bodies, substrates, and coatings include slip casting, tape casting and dipping, respectively[2-9]. The components produced by these routes can have a great variety of shapes and sizes and meet the requirements for a broad number of applications in many sectors like microelectronics, structural, biological and photocatalysis, to mention only a few[10]. The deposition of thin films of nanocomposites with colloidal particles is commonly performed by dip-coating. Dipping allows us to produce coatings with thicknesses of an order of magnitude of few microns and permits a desirable control of composition, density and hardness after sintering[5, 9, 10].

The coating of nickel matrix composites with high density and tailored microstructures having new interesting properties has been studied recently using different approaches, one of the most interesting being the use of colloidal routes[11, 12]. Several works have reported the rheology, the electrolytic properties and the interactions between phases in metal-ceramic composites with oxides as ceramic reinforcing phase, mainly Al_2O_3, SiO_2, ZrO_2 and $TiO_2$for applications as electrodes[13] for fuel cells and structural components[14]. Among the nanoparticles of the second phase mentioned above, titania is widely used as a photocatalytic agent, in biomedical devices, as well as hardening of a metallic matrix to enhance the strength and stiffness of structural components[15-18]. In this context, this work aimed to evaluate the production of composite coatings of nickel reinforced with titania nanoparticles produced by immersion in aqueous suspensions of Ni-TiO_2 mixtures without additives.

Methods

A micron sized powder of nickel (T110, INCO, Canada) and a nanotitania suspension (Aerodisp W 740X, Degussa-Evonik, Germany) with mean particle sizes of 2.5 µm and 40 nm and densities of 8.7 and 4.2 $g.cm^{-3}$ respectively, were used. Aqueous suspensions of Ni/TiO_2 mixtures with concentrations of 1.0, 3.0, and 5.0 vol.% (0.5, 1.5, and 2.5 wt%, respectively) of nanotitania were prepared to final solids contents of 30 vol.% using deionized water. According to previous studies[2] suspensions were

---

*e-mail: eloi_junior@hotmail.com

stabilized with 1 wt% commercial polyacrylic acid based polyelectrolyte (Duramax D-3005, Rohm and Haas, USA) adding tetramethyl ammonium hydroxide (TMAH) up to pH 10 to prevent degradation of the powder. Suspensions were prepared by ultrasonic mixing using a 400 W sonication probe (Dr. Hielscher U400S, Germany) for 3 min and further stirring for 1 h. Rheological characterization was carried out using a rheometer RS50 (ThermoHaake, Germany) with a double-cone/plate sensor configuration (DC60/2°, ThermoHaake, Germany) and a testing temperature of 25°C. Flow behavior was measured under controlled rate conditions employing a measuring program in three stages; first a linear increase of shear rate from 0 to $1000s^{-1}$ in 3 min; a plateau at the maximum shear rate ($1000s^{-1}$) for 30s, and a decrease to zero shear rate in 3 min.

Commercially available sheets of low carbon content steel AISI 1020 were used as coating substrates. The microstructure of the carbon steel sheet used as substrate material of the composite layer of Ni-TiO_2 is shown in Figure 1. It can be seen that it has a homogeneous microstructure with little variability in grain size comprising predominantly ferritic matrix with a few colonies of pearlite in the grain boundaries with a random distribution.

Single coatings of Ni-TiO_2 were obtained by dipping at a withdrawal rate of 10 $mm \cdot s^{-1}$. Every formed layer was weighted after 24h drying in air at room temperature. Green samples were sintered under Ar/5% H_2 flowing atmosphere using a two-step heat treatment, with a first ramp from room temperature to 500°C in 40 min to allow deflocculant burnout and a second step from 500°C to 900°C in 1 h. The final microstructure of the sintered bodies was observed by optical and scanning electron microscopy SEM (Leica DM4000M, Germany, and Phillips XK30, respectively, Netherlands). Sintered samples were observed on polished surfaces after chemical etching (Nital reagent). Present phases in the composite coating layer were identified by X-ray diffraction using a X'Pert (Philips, Netherlands) apparatus with a Cu (λ = 1.54 Å) target and a Ni filter at 0.02° (2θ/s) scanning speed. For analysis at different depths, the material was removed using fine sandpaper (1200 particles per square). Vickers hardness was determined for the coating and matrix samples using a microdurometer (Shimadzu HMV–2, Japan). The results were obtained from an average of 10 measurements.

Results and discussions

Figure 2 shows the flow curves obtained from the rheological measurements of the suspensions with a solids content of 30 vol.% and different concentrations of TiO_2. The results show that the suspensions have a pseudoplastic behavior with the presence of a negligible yield stress, which indicates that a very good dispersion condition. Another important feature is the absence of thixotropy, which allows us to assume that the deflocculation process has been successful to prevent attraction interactions (van der Waals forces) among the particles. These results are characteristic of well-dispersed suspensions with high solids concentration.

From the flow behavior the influence of the concentration of nanoparticles of titania on the viscosity of the suspensions can be drawn, as shown in Figure 3 for viscosity values taken at a shear rate of $50s^{-1}$. Observing the figure it is noted that increasing amounts of TiO_2 nanoparticles lead to a square root increase of the viscosity values. The viscosity values increase can then be attributed to the lack of affinity between the ammonium polyacrylate and organic compounds components of the titania suspension. These nanoparticles remain in the liquid medium, promoting thickening of the suspension, as it increases the concentration of nanoparticles.

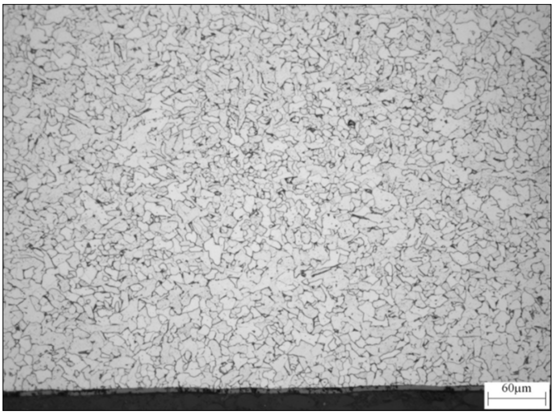

Figure 1: Steel sheet substrate before any heat treatment.

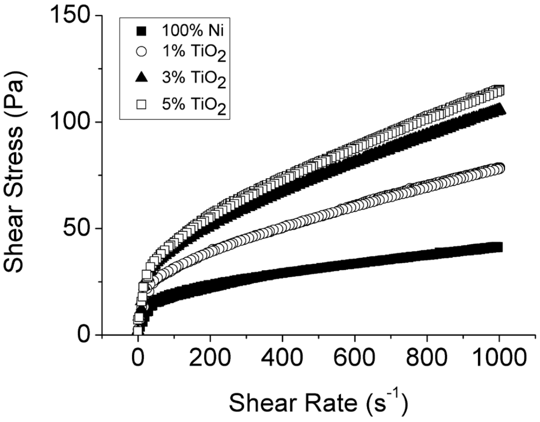

Figure 2: Flow curves of 30 vol.% suspensions of Ni-TiO_2 mixtures with different TiO_2 contents (vol.%).

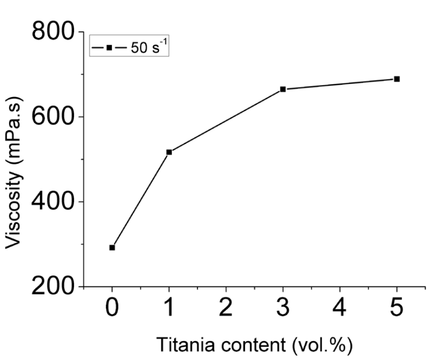

Figure 3: Apparent viscosity of the suspensions of Ni-TiO_2 mixtures with different TiO_2 contents.

Steel substrates were dip-coated with these suspensions and further sintered at 900°C/1h. After sintering, nanostructured coatings were obtained. Homogeneous, crack-free coatings with a relatively high porosity (Figure 4) were obtained in which titania nanoparticles are very well distributed around the surface of Ni particles. The microstructure may be divided into three well-defined regions as shown in the SEM pictures presented in Figure 5. The outer surface consists of a porous layer of the Ni-TiO_2 coating. The second region shows the existence of a connection interface between the composite coating and the substrate. This presents a clear path for diffusion of nickel atoms in the grain boundaries of the steel substrate during sintering. The maintenance of the sample for increasing times in the furnace enabled atoms of nickel to penetrate into the crystal lattice of iron forming the third region of the microstructure.

The substrate showed significant microstructural changes after sintering of the composite coating. As can be noted, there was an increase in grain size in the first layer of the substrate microstructure attributed to the formation of austenite (Fe-γ), characterized by coarser and polyhedral grains. The formation of this microstructure is due to the typical nickel atoms diffusion process into the iron lattice crystalline, which is accelerated by high temperature. Nickel is gammagene element which enables the presence of austenite at room temperature. Furthermore, the inferior layers of the microstructure also underwent changes due to the migration of nickel into the steel. The austenite is able to absorb carbon atoms in their crystal structure about 2.0wt%. This means that colonies of pearlite dissolve the free carbon migrate to the surface and saturate the austenite. Consequently, it can be observed an intermediate region of ferrite (Fe-α) and a combination of ferrite-pearlite composing the original microstructure of the steel[19, 20].

The high viscosity of the Ni-TiO_2 suspensions, influenced the adhesion during the formation of the coating. This effect is shown in Figure 6. Despite their high porosity the coatings with concentrations of nanoparticles of up to 3.0 vol.% showed a good adherence to the substrate (Fig. 6 (a) and (b)). However, the addition of 5.0 vol% of nanoparticles led to poor adherence and the layer peels out (Fig. 5 (c)). This lack of adherence can be explained primarily by the greater viscosity of the Ni-5%TiO_2 suspension that leads to thicker coatings and faster drying, thus affecting the anchoring on the steel surface.

Microhardness measurements were performed in different regions of the microstructure: within the coating and at the interface with the substrate. Table 1 shows the correlation between the microhardness values profile and the titania content in the Ni-TiO_2 composites for the three distinct regions of the microstructure after sintering. The first column presents measurements from the surface where the coating

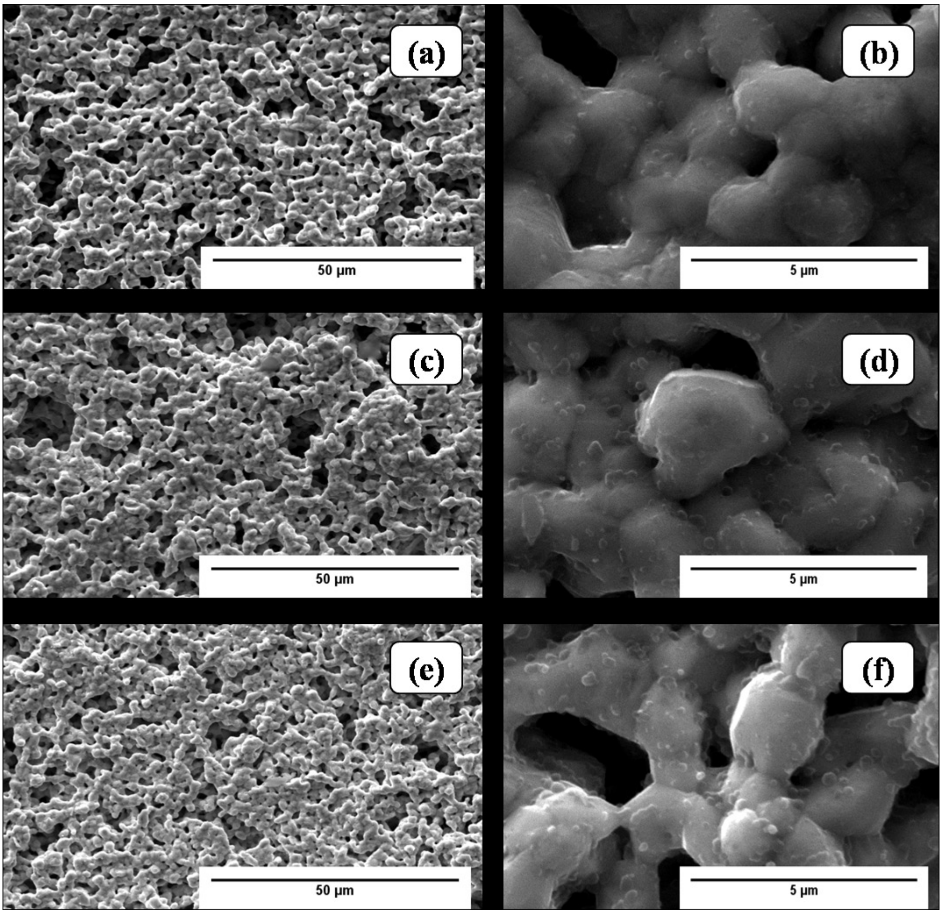

Figure 4: Microstructure of Ni-TiO_2 composite coatings at different magnification. (a,b) Ni-1%TiO_2; (c, d) Ni-3%TiO_2 and; (e, f) Ni-5%TiO_2.

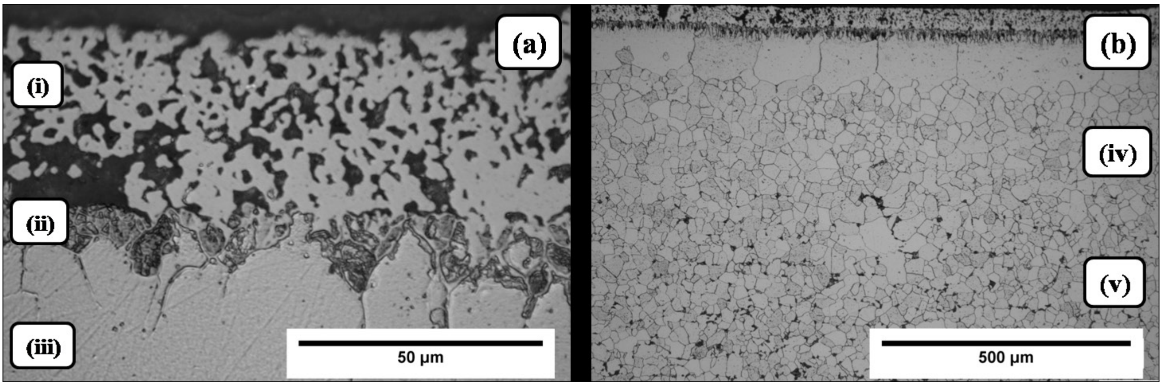

Figure 5: Microstructure distribution of the Ni-1%TiO2 composite. (a) First, second and third regions of the superficial microstructure. (i) Ni-TiO2 composite coating, (ii) Diffusion zone and; (iii) Large grains; (b) Full Ni-1%TiO2 composite microstructure. (iv) Ferrite grains and; (v) Ferrite-Pearlite grains.

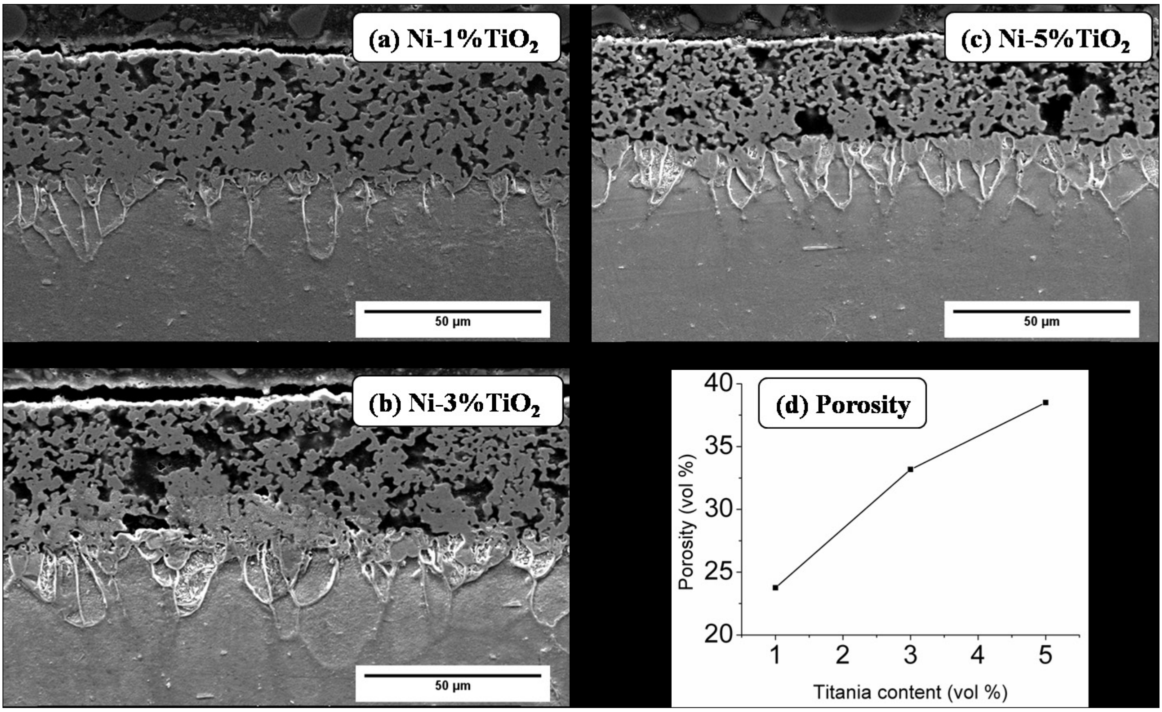

Figure 6: Influence of the nanotitania content on the adhesion of the coating and the final porosity of the Ni-TiO_2 **composites.** (a) Ni-1%TiO_2; (b) Ni-3%TiO_2; (c) Ni-5%TiO_2 and; (d) porosity evolution according to the nano-TiO_2 content.

is situated. It is evident that the increase of the values is due to the increasing concentration of nanoparticles, since the coating has high porosity and influence of this factor is already being considered in the measurement. The second column refers to the intermediate layer adhered to the substrate. The results show that there was a tendency of the hardness to decrease with increasing titania content. This can be explained correlating the amount of coverage provided to the nanoparticles over nickel particles. These results suggest that the higher the concentration of nanoparticles promotes a thicker nanotitania coating and consequently, the lowest rate of diffusion of nickel into the steel matrix carbon. Finally the results obtained for the substrate show that it was not affected by the composite coating.

To identify the phases present in the microstructure the sintered samples were analysed by X-ray diffraction following this methodology: first, the surface layer was scanned and made some removal of material by grinding and new scans were further made. The results are shown in Figure 7. Figure 7a shows all grouped diffractograms. The peaks of Fe and Ni are mixed with each other because they are very close. The sintering process promoted the composite coating consolidation and performs a mechanism of homogenization and formation of intermediate phases. Firstly, in the first

Table 1. Vickers microhardness values of the Ni-TiO_2 composites.

TiO_2 content (vol. %)	Vickers hardness (GPa)		
	Coating	Interface	Substrate
1	0.77 ± 0.03	1.77 ± 0.20	1.05 ± 0.01
3	0.80 ± 0.08	1.70 ± 0.48	1.04 ± 0.01
5	0.89 ± 0.05	1.63 ± 0.24	1.07 ± 0.01

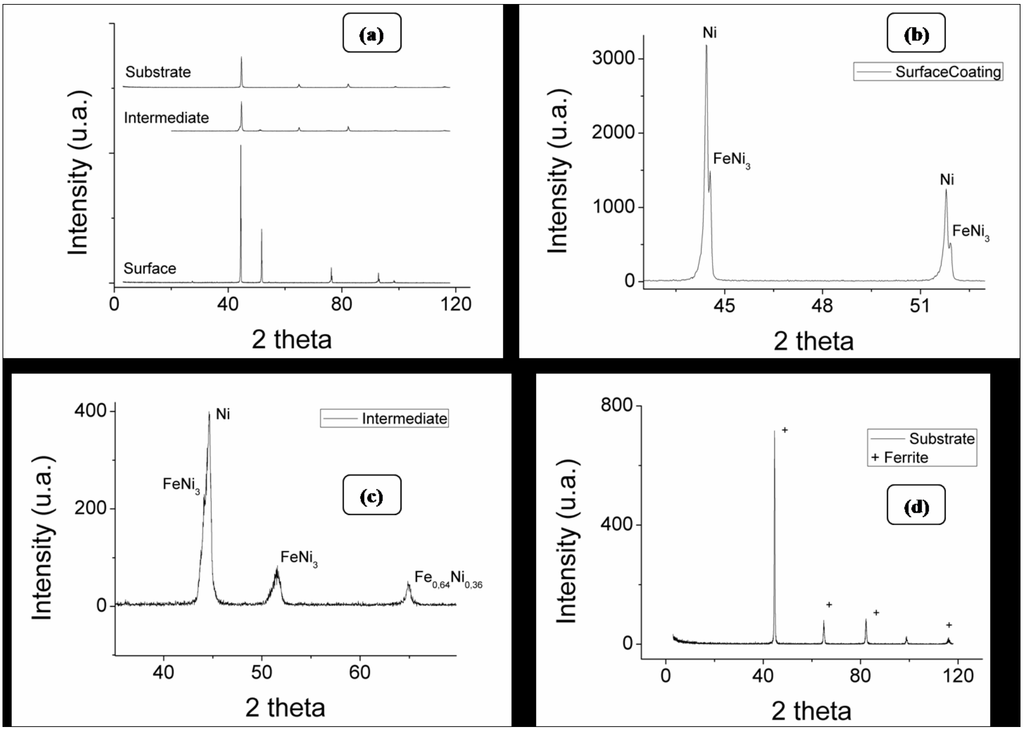

Figure 7: X-Ray diffraction. (a) Whole sample; (b) Surface coating; (c) Second layer; and (d) Substrate.

layer, peaks were identified as pure nickel and a nickel-rich intermetallic compound $FeNi_3$ (Figure 7b). In a lower region, between the coating and the substrate, the formation of a stoichiometric compound rich in iron, $Fe_{0,64}Ni_{0,36}$ (Figure 7c), which is not present in the equilibrium phase diagram can also be identified. With further grinding only Fe peaks were observed (Figure 7d). Finally, the peaks of pure nickel show a slight enlargement. This can be attributed to the formation of substitutional solid solution from the migration of iron atoms to the crystalline lattice of the nickel.

Conclusions

A study of the dip-coating process of low carbon steel plated with Ni-TiO_2 composite by colloidal route was made. The results obtained from the rheological behavior showed that the viscosity of the suspensions increases in the presence of nanoparticles. The final microstructure obtained was divided into three regions: the coating showed the TiO_2 nanoparticles covering the Ni particles. The formation of an interface comprising Fe-Ni was formed during sintering. In this case, the nanoparticles promote a reduction in the diffusivity of atoms of nickel to the substrate during the sintering step. In the third region, i.e. the substrate, the observed formation of a layer of coarse grains suggests that it is formed by austenite. This region has absorbed carbon contained in the pearlite microstructure of steel, changing the final microstructure of the substrate, which shows coarse grains, a ferritic region and finally again the presence of perlite. The microhardness value obtained slightly changed between the different regions. The coating obtained the lowest results, the substrate showed intermediate values similar to those of uncoated substrates, whereas the highest values were obtained at the interface, which is related to the formation of a compound of the Fe-Ni substitutional solid solution.

Aknowledgements

This work has been supported by CNPq (National Council for Scientific and Technological Development, Brazil).Authors greatly acknowledge the financial Support of CAPES in the frame of the International Cooperation Program Science without Borders for Special Visiting Researcher PVE (MEC/MCTI/CAPES/CNPq/FAPs/ Nº71/2013), Project Nº A011/2013.

References

1. Ferreira JM. *Tecnologia da Pulvurometalurgia*. Lisboa: Federação Calouste Gulbekian; 2002.
2. Sánchez-Herencia AJ, Millán AJ, Nieto MI, Moreno R, Aqueous colloidal processing of the nickel powder. *Acta Materialia*. 2001;49(4):645-651. doi:10.1016/S1359-645400)00347-5
3. Rosso M. Ceramic and metal matrix composites: Routes and properties. *Journal of Materials Processing Technology*. 2006;175(1-3):364-375. doi:10.1016/j.jmatprotec.2005.04.038
4. Ferrari B, Moreno R. Ni-YSZ graded coatings produced by dipping. *Advanced Engineering Materials*. 2004;6(12):969-971. doi: 10.1002/adem.200400116
5. Canut B, Blanchin MG, Teodorescu V, Traverse A. Structure of Ni/SiO_2 films prepared by sol–gel dip coating. *Journal of Non-Crystalline Solids*. 2007;353(27):2646-2653. doi:10.1016/j.jnoncrysol.2007.05.009
6. Castro AL, Liborio JB, Pandolfelli VC. Reologia de concretos de alto desempenho aplicados na construção civil - Revisão. *Cerâmica*. 2011;57(341):63-75. doi: 10.1590/S0366-69132011000100009
7. Ferrari B, Sánchez-Herencia AJ, Moreno R. Nickel-alumina graded coating obtained by dipping and EPD on nickel substrates. *Journal of the European Ceramic Society*. 2006;26(12): 2205-2212. doi:10.1016/j.jeurceramsoc.2005.04.009
8. Hotza D. Artigo revisão: Colagem de Folhas Cerâmicas. *Cerâmica*. 1997;43(283-284):157-164. doi: 10.1590/S0366-69131997000400002
9. Brinker CJ, Frye GC, Hurd AJ, Ashley CS. Fundamental of sol-gel dip coating. *Thin Solid Films*. 1991;201:97-108.
10. Rahaman MN. *Ceramic processing and sintering*. 2a ed. New York: Marcel Drekker; 1995.
11. Novakovic J, Vassiliou P. Vacuum thermal treated electroless NiP–TiO_2 composite coatings. *Electrochimica Acta*. 2009;54(9):2499-2503. doi:10.1016/j.electacta.2008.12.015
12. Aal AA, Hassan HB, Rahim MA. Nanostructured Ni–P–TiO_2 composite coatings for electrocatalytic oxidation of small organic molecules. *Journal of Electroanalytical Chemistry*. 2008;619-620:17 -25. doi:10.1016/j.jelechem.2008.03.004
13. García P, Ferrari B, Moreno R, Sánchez-Herencia AJ, Colomer MT. YSZ/Ni–YSZ semi-cells shaped by electrophoretic deposition. *Journal of the European Ceramic Society*. 2007;27(13):4241-4244. doi:10.1016/j.jeurceramsoc.2007.02.142
14. Sánchez-Herencia AJ, Hernández N, Moreno R. Rheological behavior and slip casting of Al_2O_3–Ni aqueous suspensions. *Journal of the American Ceramic Society*. 2006;89(6):1890 -1896.
15. Vieira Jr. LE, Rodrigues Neto JB, Klein AN, Bhandarkar S, Hotza, D, Moreno, R. Rheological and structural characterization of Ni–SiO_2 nanocomposites produced by aqueous colloidal processing. *Journal of the American Ceramic Society*. 2011;94(12):4179- 4183. doi: 10.1111/j.1551-2916.2011.04754.x
16. Lin CS, Lee CY, Chang CF, Chang CH. Annealing behavior of electrodeposited Ni-TiO_2 composite coatings. *Surface & Coatings Technology*. 2006;200(12-13):3690-3697. doi:10.1016/j.surfcoat.2004.10.001
17. Shibli SM, Dilimon VS. Effect of phosphorous content and TiO_2-reinforcement on Ni–P electroless plates for hydrogen evolution reaction. *International Journal of Hydrogen Energy*. 2007;32(12):1694-1700. doi:10.1016/j.ijhydene.2006.11.037
18. Zhao L, Bram M, Buchkremer HP, Stöver D, Li Z. Preparation of TiO_2 composite microfiltration membranes by the wet powder spraying method. *Journal of Membrane Science*. 2004;244(1-2):107-115. doi:10.1016/j.memsci.2004.07.010
19. ASM. *Metals Handbook - Alloy Phase Diagrams*. [S.l.]: ASM International; 1992. v. 3.
20. Chiaverini V. *Aços e Ferros Fundidos*. 6a ed. São Paulo: ABM; 1988.